Storey-based stability of multi-storey steel semi-braced and unbraced frames with semi-rigid connections

Terence Ma[1], Lei Xu[2]

[1] PhD Graduate, Department of Civil and Environmental Engineering, University of Waterloo, 200 University Avenue West, Waterloo, ON., N2L 3G1, Canada

[2] Professor, Department of Civil and Environmental Engineering, University of Waterloo, 200 University Avenue West, Waterloo, ON., N2L 3G1, Canada

Corresponding Author:
Lei Xu, University of Waterloo
200 University Avenue West
Waterloo, ON. N2L 3G1
Email: lxu@uwaterloo.ca

Abstract

A simplified method is proposed for evaluating the stability of multi-storey, steel semi-braced and unbraced frames with semi-rigid connections. The proposed method decomposes a frame into individual storeys and evaluates the lateral stiffness of each storey via the storey-based stability approach with explicit, closed form solutions. Lateral sway instability occurs when the lateral stiffness of any storey diminishes to zero, and the storey for which this occurs can be considered the weakest storey in the frame. The results of the proposed method are theoretically verified via comparison to the results of finite element analyses. Use of the proposed decomposition method requires assuming the buckled shape of the frame, which is shown to provide satisfactory approximations of critical loads for engineering practice. Parametric studies are conducted to assess the sensitivity of the results to the corresponding buckling shape parameters. The assumption of asymmetric buckling, which is generally consistent with the sway buckling mode in semi-braced frames, produces reliable results in the proposed decomposition method.

Keywords: stability, steel frames, multi-storey, proportional loading, sway, buckling, storey-based

https://ascelibrary.org/doi/10.1061/%28ASCE%29ST.1943-541X.0002874

1 Introduction

In current practice, the analysis of multi-storey structures is commonly completed in design by assessing the capacity of the individual members. However, in reality the members often interact especially when semi-rigid or rigid connections exist. The holistic consideration of individual storeys within multi-storey buildings as entire structural systems of framing members is more realistic as it accounts for these interactions between members and may result in more cost-effective design solutions. The consideration of overall stability in a structure can also be overlooked when the members are considered individually. Designers may alternatively opt to choose among the many existing advanced computer models for evaluating the stability of structures. However, it can be difficult for users to verify or interpret the results in sophisticated analysis packages. The numerical procedures and computational algorithms often employed by modern programs can be difficult for normal practitioners to understand, and seem like black boxes that are prone to technical glitches or inaccurate results if the users employ the wrong assumptions during creation of the models.

Presented in this paper is a storey-based method for evaluating the stability of multi-storey frames with semi-rigid connections. The proposed method is a much more simplistic and meaningful representation of the solution of the problem, presented in closed form, while also considering global stability via the interaction of rotational stiffness between stories. All of the variables in the proposed equations have physical meanings which can be easy to understand for users.

The scope of this study is limited to semi-braced and unbraced frames. Semi-braced frames are defined as those with limited amounts of lateral bracing present but still experience significant lateral sway in the buckling mode (Ma 2020). Unbraced frames have no lateral bracing present and similarly experience lateral sway in the buckling mode. Semi-braced frames also tend to have critical loads between the values obtained by either removing the bracing or providing infinite bracing. As the use of semi-rigid connections is becoming more popular in practice (Bahaz et al. 2017), the method can be applied towards both semi-rigid and idealized pinned and rigid connections.

The method supersedes the storey-based stability approach of decomposition originally developed by Liu and Xu (2005) and applied in Xu and Wang (2007), which also involves the decomposition of frames into individual storeys and evaluating the lateral stiffness of each storey. In simple terms, the decomposition process involves replacing members with equivalent rotational springs at the ends of their connecting members until only the columns within a single storey of the frame remain. In short, the Liu and Xu (2005) method is not realistic as it neglects part of the

beam contribution to the rotational stiffness at the column ends, resulting in inaccurate solutions. Closed-form and explicit equations are derived in this paper to appropriately consider the rotational stiffness interactions between upper and lower columns in sway frames, which significantly affect the end conditions of columns (Bridge and Fraser 1987; Hellesland and Bjorhovde 1996; Webber et al. 2015; Meghezzi-Larafi and Tati 2016; Li et al. 2016). In addition, the effect of axial forces on both lateral and rotational column stiffness are considered, and is also known to significantly affect stability analyses (Bridge and Fraser 1987). The consideration of semi-braced frames is also included in addition to the unbraced frames studied in Liu and Xu (2005).

The proposed method is based on the fact that instability in a frame occurs when the lateral stiffness of any one storey diminishes to zero has been adopted in many previous formulations of storey-based stability. This was expressed explicitly in the single-storey-stability methods of Xu (2001) and Xu and Liu (2002), storey-decomposition method (Liu and Xu 2005), and further extensions of the storey-based stability method to account for column imperfections (Ma and Xu 2019a), temperature (Ma and Xu 2019b) and shear deformations (Ma & Xu 2019c). As such, the critical loads of a frame can be determined using the proposed method under various proportional loading schemes via root finding. Moreover, the storey which first reaches zero lateral stiffness can be considered to be a weak storey (Teresa Guevara-Perez 2012; Bahaz et al. 2017). The proposed method is shown to be theoretically accurate via comparison to the results of finite element analysis (FEA). As the proposed method also requires assuming the buckled shape of the frame at the critical loads, the results of a parametric study on the sensitivity of the obtained critical loads to the proposed buckling shape parameters are presented to validate the buckled shape for engineering practice.

2 Background

The storey-based stability approach was initially proposed by Yura (1971). It involves considering the simultaneous lateral buckling of all columns in a storey rather than the individual buckling loads of the columns. The approach is useful as it considers the interactions among all members in a storey, which are neglected in analysis methods of individual member capacity such as the alignment chart method which is widely adopted in structural design standards (CSA 2014; AISC 2017). These interactions have been shown to have significant effects, both beneficial and detrimental to the buckling loads of members (Bridge and Fraser 1987; Hellesland and Bjorhovde 1996; Webber et al. 2015; Meghezzi-Larafi and Tati 2016; Li et al. 2016). The approach was continually developed over the next few decades. LeMessurier (1977) and Lui (1992) subsequently used the concept to develop matrix-based methods

for evaluating storey-based stability. Following this, Xu (2001) and Xu and Liu (2002) developed closed-form equations for evaluating storey-based stability. Xu (2001) proposed a method to evaluate the storey-based stability of a single storey frame with considering the effect of axial force on the lateral stiffness of a member, whereby the lateral stiffness of a single unbraced storey frame, ΣS, is given in Eq. (1), and represents the instantaneous ratio of force to lateral displacement in the storey.

$$\Sigma S = \sum_{j=1}^{n} S_{\Delta,j} = \sum_{j=1}^{n}\left[\frac{12E_{c,j}I_{c,j}}{L_{c,j}^3}\beta_j(\phi_j, r_{l,j}, r_{u,j})\right] \tag{1a}$$

$$\beta = \frac{\phi^3}{12}\left[\frac{a_1\phi\cos\phi + a_2\sin\phi}{18r_l r_u - a_3\cos\phi + (a_1 - a_2)\phi\sin\phi}\right] \tag{1b}$$

$$a_1 = 3[r_l(1-r_u) + r_u(1-r_l)] \tag{1c}$$

$$a_2 = 9r_l r_u - (1-r_l)(1-r_u)\phi^2 \tag{1d}$$

$$a_3 = 18r_l r_u + a_1\phi^2 \tag{1e}$$

In Eq. (1), $\phi = L_c(N_c/E_cI_c)^{0.5}$ is the axial load coefficient of a column, and n is the number of columns in the frame. The properties E, I and L refer to the modulus of elasticity, moment of inertia and length, respectively, and the subscript c relates to the columns of the frame. N_c is the axial compressive force in the column. $S_{\Delta,j}$ is the lateral stiffness of column j. r_u and r_l are the end fixities of the upper and lower ends of the columns, respectively, obtained via Eq. (2) (Monforton and Wu 1963).

$$r = \frac{1}{1+3EI/RL} \tag{2}$$

In Eq. (2), R is the total rotational stiffness of the members connected to the corresponding end of the column. The value of r ranges between zero for pinned connections and unity for fixed connections. The value of β is positive if the column can withstand its axial load by itself. $\beta = 0$ corresponds to the instance during which the column no longer offers resistance and begins to lean on the system. It can also be negative, which indicates that the column relies on the lateral stiffness of other columns in the storey in order to maintain stability. Further background information regarding the behaviour of this coefficient is included in Appendix A. The storey is considered unstable when ΣS diminishes to zero. Note that the use of Eqs. (1) requires the assumption that the upper ends of the columns in the frame experience the same lateral deflection, which is valid for the assumption of rigid floor and roof systems (Xu 2001). This idealization also neglects the diaphragm rotation which, to some degree, may be present in real structures.

In an attempt to extend the storey-based stability method towards multi-storey analysis, Liu and Xu (2005) proposed a method to decompose the frames into a series of single storey frames, each to be analyzed separately using the Xu (2001) method. The process of decomposing a multi-storey frame into individual storeys is illustrated in Fig. 1 below, whereby the columns and beams connected to each end of each column in storey i (shown with dashed lines) are replaced with equivalent springs of rotational stiffness R_u and R_l. The values of R_u and R_l can subsequently be transformed into the end fixity factors, r_u and r_l, via Eq. (2) for use in Eq. (1). If the lower end of the column is attached to the base foundation then R_l is the rotational stiffness of the base connection.

Fig. 1. Illustration of decomposition model for general multi-storey frame

The decomposition procedure can be completed for each storey, and instability occurs when the lateral stiffness, ΣS, in Eq. (1) for any single storey diminishes to zero (Liu and Xu 2005). Columns that have negative values of S_Δ rely on other columns to remain stable (Xu 2001). The value of the column end rotational stiffness, R (either R_u or R_l), was proposed in Liu and Xu's (2005) as Eq. (3).

$$R = \sum_{k=1}^{n_{conn}} \mu_k R_k^{'} \tag{3a}$$

$$R_k^{'} = \frac{6E_k I_k z_{N,k}}{L_k (4 - z_{N,k} z_{F,k})} \left(2 + v_{FN,k} z_{F,k}\right) \tag{3b}$$

In Eq. (3), n_{conn} is the number of members (beams and columns) connected at the corresponding end of the column for which R is being evaluated, and R'_k is the equivalent rotational stiffness provided by member k at the corresponding connection. $z_{N,k}$ and $z_{F,k}$ are the near-end and far-end member-connection fixities of the k^{th} connected member, calculated in Eq. (4) with Z being the rotational stiffness of the corresponding connection. A pinned connection has $Z = 0$ and $z = 0$ while a rigid connection has $Z = \infty$ corresponding to $z = 1$.

$$z_{N,k} = \frac{1}{1 + 3E_k I_k / (Z_N L_k)} \tag{4a}$$

$$z_{F,k} = \frac{1}{1 + 3E_k I_k / (Z_F L_k)} \tag{4b}$$

The member-connection fixity factor, z, is similar to the end fixity factor in that it ranges from zero to unity, but quantifies the rotational stiffness of the actual connection between two adjoining members (Z) rather than the equivalent rotational stiffness to the end of column provided by adjoining members or ground connections (R). To illustrate this difference, a column whose upper end is rigidly connected to other deformable members will have a finite value of R_u since its upper end will rotate, but $Z_u = \infty$ since the connection is rigid. $v_{FN,k}$ is the ratio of far-end

to near-end connection rotations of the k^{th} connected member, based on the assumed deformed shape of the frame, corresponding to the buckling mode. According to Liu and Xu (2005), if member k is a beam, then μ_k is a distribution factor that partitions R'_k to the two column ends joined at their connection with the beam, based on the relative stiffness of the columns. If member k is a column then $\mu_k = 1$ since partitioning is only applicable for the beams (Liu and Xu 2005). For beams, μ_k is expressed in Eq. (5).

$$\mu_k = \frac{R_c^{'}}{R_c^{'} + R_{c'}^{'}} \tag{5}$$

In Eq. (5), R'_c is the rotational stiffness of column for which R is being calculated and $R'_{c'}$ is the rotational stiffness of the other connecting column at the joint, both obtainable via Eq. (3b). However, Eq. (3b) neglects the effect of column axial loads towards reducing the rotational stiffness of the contributing column, and thus overestimates the end rotational stiffness contribution of columns. Moreover, the derivation for Eq. (3b) neglects the differential lateral displacement (DLD) between the ends of member k (Monforton and Wu 1963). In the sway buckling mode, which generally governs in semi-braced and unbraced frames and corresponds to the failure mode detected in the storey-based stability method (Xu 2001), this differential lateral displacement of the columns cannot be neglected, as the analysis would otherwise correspond to that of a braced frame. That is, DLD occurs in the columns of unbraced and semi-braced frames, but not in braced frames. Finally, the use of the distribution factor, μ_k, in Liu and Xu (2005) is not realistic as it is based on an assumption that all columns reach their individual buckling loads simultaneously with the ends of the members in the frame rotating by the same magnitude (Duan and Chen 1999), and neglects a portion of the beam contribution to the column end rotational stiffness. As the decomposition of a frame into individual storeys requires replacing all of the members immediately connected to the columns in a given storey with equivalent rotational springs (as shown in Fig. 1), the total rotational stiffness of the members being replaced should be considered rather than just a portion, μ_k, thereof. Unlike the Liu and Xu (2005) method, in the proposed method, the end fixity factors of the columns in a storey are obtained by calculating R as the summation of the rotational stiffness of all connected members at the column end without using the distribution factor, μ_k. The column-to-column end rotational stiffness contribution is properly accounted for via a derivation of the rotational stiffness with considering both the axial load and chord rotation experienced by the connected column. It is demonstrated via finite element analysis that the proposed equations yield exact results of these values using these modifications.

It is also noted that apart from Liu and Xu (2005), a number of other studies have been conducted on the stability of multi-storey steel frames. Similar stability methods (Georgios and Gantes 2006; Webber et al. 2015; Meghezzi-Larafi and Tati 2016; Gunaydin and Aydin 2019) have isolated columns in multi-storey frames for individual effective length analysis, with accounting for rotational stiffness interactions with connecting members. However, the determination of effective length of separate columns does not consider the lateral stiffness interactions between columns of the same storey and often requires very complicated solutions. Hellesland (2009) proposed an approximate storey-based analysis method to evaluate the second-order effects relating to column imperfections (which do not affect stability according to Ziemian (2010) and Ma and Xu (2019a)) on the deformations of storeys within multi-storey frames. Finite element analysis and matrix methods have also been proposed by Kim and Choi (2015) and Li et al. (2016) for the storey-based analysis of frames, but require matrix-based solutions instead of providing closed-form, explicit solutions. Overall, the idea of decomposing a frame into individual storeys to be analyzed for instability corresponding to zero lateral stiffness is easy to understand but has only been addressed by Liu & Xu (2005), in which the aforementioned shortcomings result in only approximate equations unlike the equations in the proposed method. Nevertheless, approximations can be useful if accurate results can still be produced. In particular, it has been widely demonstrated in previous studies of storey-based stability (Xu and Liu 2002; Liu and Xu 2005; Li et al. 2016; Ma and Xu 2019a; Ma and Xu 2019c) that the buckled shapes of the frames are not readily pre-determinable and need to be assumed in the proposed method. The diminishing of the lateral stiffness to zero in a semi-braced or unbraced frame corresponds to the sway buckling mode (Xu 2001) and the asymmetrical buckling mode generally governs for sway frames (Bažant and Xiang 1997). As such, the case of asymmetrical buckling has been commonly assumed to determine the buckling lengths of columns (Duan and Chen 1999; Gil-Martín and Hernández-Montes 2012), required bracing stiffness (Bažant and Xiang 1997), as well as in storey-based stability analysis (Xu and Liu 2002). As consistent with the aforementioned studies on storey-based stability, this assumption was found to closely approximate the critical loads in the proposed method as well.

3 Decomposition of an *m*-storey Frame into Individual Storeys

Consider first the continuous column within the span of a single storey, located in a planar multi-storey frame shown in the left of Fig. 2. The columns in the frame are indexed from left to right as j from 1 to n, and the storeys indexed from bottom to top as i from 1 to m. Also, the subscripts c and b will refer to the properties of the columns and beams, respectively.

Fig. 2. Schematic of typical column in multi-storey frame

3.1 End Fixity Factors

Column (*i,j*) has upper and lower end fixities $r_{u,i,j}$ and $r_{l,i,j}$, which are determined via Eq. (2). The values of *R* in Eq. (2) are influenced by axial forces in the connected members shown in dashed grey lines to the right of Fig. 2, which are represented in Fig. 3. The connected members provide rotational restraint to the ends of column (*i,j*), which can be quantified using the end fixity factors via Eq. (2). As shown to the right of Fig. 2, the member in Fig. 3 representing a connected beam or column will be replaced by equivalent rotational springs at the ends of the columns that it is connected to. Note that Fig. 3 is similar to the one used in the derivation of Monforton and Wu (1963) except that it is subjected to an axial load *N*. Its end moments are M_A and M_B, and the subscripts *A* and *B* correspond to the respective ends of the member. The transverse reactions Y_A and Y_B are also present at the ends. As consistent with traditional stability analysis, loads are assumed to be applied only at the joints of the frame (Yura 1971; Xu 2001; Xu and Liu 2002).

Fig. 3. Deformation of a typical member with considering axial load effects

The transverse displacement is denoted by *y* and the chord rotation is simply the change to the angle between the ends of the member. θ is the rotation at the ends of the semi-rigid member, while Φ is the connection rotation at each end. To be clear, a semi-rigid member is defined as consisting of the flexurally-deformable portion with *EI* as well as the connections shown in Fig. 3. As such, the rotation at the ends of the flexurally-deformable portion is θ-Φ. By applying the external equilibrium of forces and moments, the following relations can be obtained.

$$Y_B = -Y_A \tag{6a}$$

$$M_A + M_B + N(y_B - y_A) + Y_B L = 0 \tag{6b}$$

M_A and M_B are expressed as the following functions of the end connection rotation stiffness, Z_A and Z_B.

$$M_A = \Phi_A Z_A \tag{7a}$$

$$M_B = \Phi_B Z_B \tag{7b}$$

The internal bending moment in the member in Fig. 2 is expressed via the Euler-Bernoulli equation in Eq. (8). Shear deformations are neglected as they are generally insignificant for members of typical slenderness.

$$-EIy'' = N(y(x) - y_A) + M_A - Y_A x \tag{8}$$

Substituting Eq. (6a) and Eq. (7a) into Eq. (8) and solving the differential equation for *y* yields Eq. (9).

$$y(x) = y_A + C_1 \cos\left(\frac{\phi}{L}x\right) + C_2 \sin\left(\frac{\phi}{L}x\right) - \frac{\Phi_A Z_A}{N} - \frac{Y_B}{N}x \tag{9}$$

There are four boundary conditions for Eq. (9), listed below.

$$y(0) = y_A \tag{10a}$$

$$y(L) = y_B \tag{10b}$$

$$y'(0) = \theta_A - \Phi_A \tag{10c}$$

$$y'(L) = \theta_B - \Phi_B \tag{10d}$$

Substituting Eqs. (10) into Eqs. (9) and Eqs. (7) into Eq. (6b) yields a system of five linear equations in terms of the coefficients C_1 and C_2, the connection rotations Φ_A, Φ_B, and Y_B. As such, system of equations can be solved to express the above five variables (C_1, C_2, Φ_A, Φ_B, and Y_B) in terms of all other variables. The solutions for Φ_A and Φ_B can be multiplied by Z_A and Z_B, respectively, to express the end moments in Eq. (7) as linear equations with respect to θ_A, θ_B, y_A and y_B in Eq. (11).

$$\begin{bmatrix} M_A \\ M_B \end{bmatrix} = \begin{bmatrix} Z_A & 0 \\ 0 & Z_B \end{bmatrix} \begin{bmatrix} \Phi_A \\ \Phi_B \end{bmatrix} = \mathbf{C}_{2\times4} \begin{bmatrix} \theta_A \\ \theta_B \\ y_A \\ y_B \end{bmatrix} \tag{11}$$

In Eq. (11), $\mathbf{C}_{2\times4}$ is a rotational stiffness coefficient matrix formed by arranging the solutions of $Z_A\Phi_A$ and $Z_B\Phi_B$ into linear combinations of θ_A, θ_b, y_A and y_B. Transforming Z_A and Z_B into the member-connection fixity factors in Eq. (4) and then dividing Eq. (11) by θ_A yields the following result for $R_A = M_A/\theta_A$, which is the equivalent rotational stiffness provided to a connecting member at end A.

$$R_A^{'} = \frac{3EIz_A\phi}{L}\left[\frac{(1-z_B)\phi^2\sin\phi(1-w_{BA}) + 3z_B\left(\sin\phi(1-v_{BA}) - \phi\cos\phi(1-w_{BA}) + \phi(v_{BA}-w_{BA})\right)}{18z_Az_B + (a_1-a_2)\phi\sin\phi - a_3\cos\phi}\right] \tag{12}$$

In Eq. (12), z_A and z_B are the member-connection fixity factors of the member in Fig. 3, $\phi = L(N/EI)^{0.5}$ is the axial load coefficient of the member, a_1, a_2 and a_3 are given in Eq. (1c) through (1e) except with the end fixity factors replaced with z_A and z_B, and the shape coefficients corresponding to the deformed shape of the frame, v_{BA} and w_{BA}, are defined in Eq. (13), where v_{BA} is the ratio between end rotations at B and A, while w_{BA} is the ratio between the chord rotation and the rotation of end A.

$$v_{BA} = \theta_B / \theta_A \tag{13a}$$

$$w_{BA} = \psi / \theta_A = \frac{y_B - y_A}{L\theta_A} \tag{13b}$$

The subscripts A and B should be replaced by the appropriate subscripts corresponding to the ends of the member. The exact values of v_{BA} and w_{BA} can be expressed as functions of the relative stiffness of the adjoining members on either end of the member in Fig. 2, derived in Appendix B. However, there is no closed form solution to solve for

the shape coefficients as they are complicated transcendental functions of the end fixity factors of the adjoining members. Alternatively, the shape coefficients corresponding to the critical loading condition can be estimated by assuming the buckled shape of the frame, discussed in Section 3.4 and shown provide accurate approximations of the results in Section 5, as well as in the literature (Xu & Liu 2002; Li et al. 2016). It should also be noted that in the absence of axial loading (N = 0), Eq. (12) converges to the linear analysis equation derived by Monforton and Wu (1963), shown in Eq. (14).

$$\lim_{\phi \to 0} R_A^{'} = \frac{6EIz_A}{L(4 - z_A z_B)} \left[2 + z_B v_{BA} + (2 + z_B) w_{BA} \right] \tag{14}$$

Eq. (14) is similar to Eq. (3b) proposed in Liu and Xu (2005) except that Eq. (3b) neglects the chord rotation via w_{BA} = 0, which should not be neglected for columns buckling in the lateral sway mode. Finally, the rotational stiffness provided to the member connected at end B, R'_B, can be obtained by swapping the subscripts A and B in Eq. (12) and Eq. (14). Thus, the values of R in Eq. (2) for column (i,j) can be expressed via Eq. (15).

$$R = \sum_{k=1}^{n_b} R_{b,k}^{'} + R_c^{'} \tag{15a}$$

$$R_{b,k}^{'} = \frac{6E_{b,k} I_{b,k} z_{N,k}}{L_{b,k} (4 - z_{N,k} z_{F,k})} \left[2 + z_{F,k} v_{FN,k} + (2 + z_{F,k}) w_{FN,k} \right] \tag{15b}$$

$$R_c^{'} = \frac{3E_c I_c z_N \phi}{L_c} \left[\frac{(1 - z_F)\phi^2 \sin\phi (1 - w_{FN,c}) + 3z_F \left(\sin\phi (1 - v_{FN,c}) - \phi \cos\phi (1 - w_{FN,c}) + \phi (v_{FN,c} - w_{FN,c}) \right)}{18 z_N z_F + (a_1 - a_2)\phi \sin\phi - a_3 \cos\phi} \right] \tag{15c}$$

In Eq. (15), n_b is the number of beam ends connected to the corresponding column end and $R'_{b,k}$ is the rotational stiffness of the connected beam k. The subscripts b and c correspond to the properties of the connected beams and columns, respectively. The subscripts F and N correspond to the far and near ends of the connected member with respect to the connection, respectively. Eq. (15b) is the first-order elastic stiffness since the beams are assumed not to be axially loaded. As consistent with Xu (2001) and required in order to use Eq. (1), the beams are also assumed to be axially rigid. R'_c in Eq. (15c) is the rotational stiffness of the connected column, which considers that the columns are axially loaded. Note that Liu & Xu (2005) propose the following equation for R'_c, which differs significantly from Eq. (15c) because the corresponding derivation for Eq. (16) neglects the presence of lateral reactions at the ends of the connecting column.

$$R_c^{'} = \frac{E_c I_c}{L_c} \times \frac{3R_F L_c / (E_c I_c) - \phi_c \tan\phi_c}{1 + \frac{R_F L_c}{E_c I_c} \left(\frac{\tan\phi_c}{\phi_c} \right)} \tag{16}$$

In Eq. (16), R_F is the rotational stiffness of the far end of the column. It will be shown in Section 4.1.1 that Eq. (15c) is theoretically accurate, while Eq. (16) is inaccurate. Anyway, a couple simplifications can be made to Eqs. (15). First, the effect of differential axial shortening between adjacent columns can be neglected, resulting in $\psi = 0$, and therefore, $w_{FN,b} = 0$ for all beams in Eq. (15b). Secondly, with assuming that all column splices are continuous, $z_F = z_N = 1$ in Eq. (15c). Even at the bottom and upper ends of continuous columns, $z = 1$ should be taken, because the rotation of the corresponding end of the column is equal to that of the equivalent rotational spring produced by summing the rotational stiffness contributed by the other connected members at that end (with stiffness R_u or R_l). In other words, the end of the column is technically fixed to the equivalent rotational spring representing the decomposed members at that end. Anyway, the end fixity factors of the columns in the frame in Fig. 1 can be obtained by substituting R from Eq. (15a) into Eq. (2).

3.2 Lateral Bracing

For semi-braced frames, it is demonstrated in Xu and Liu (2001) that the lateral stiffness of bracing $K_{b,i}$ in storey i can be added to the total lateral stiffness of that storey via Eq. (17).

$$(\Sigma S)_i = \sum_{j=1}^{n} S_{\Delta,i,j} + K_{b,i} \tag{17}$$

As with Eq. (1), Eq. (17) assumes that all of the columns in the frame have the same deflection. In a multi-storey frame, Eq. (17) is valid as long as the lateral bracing stiffness K_b is only related solely to the deformation of its corresponding storey.

3.3 Inelastic Buckling

To approximately account for inelastic buckling, the elastic modulus E_c may be adjusted using empirical relations such as that proposed by Yura and Helwig (2005), presented in Eq. (18) below.

$$E = \tau E_0; \quad \tau = \begin{cases} 1 & ; \quad N/N_y < 1/3 \\ -7.38(N/N_y)\log_{10}(1.176N/N_y) & ; \quad N/N_y \geq 1/3 \end{cases} \tag{18}$$

In Eq. (18), $N_y = Af_y$ is the yielding load, N is the axial load, A is the cross-sectional area of the column, and f_y is the yield stress. If this approach is used, then failure occurs when the lateral stiffness of any storey in Eq. (17) diminishes to zero with the reductions in Eq. (18) applied. This model is commonly used in design codes (CSA 2014; AISC 2017).

Note that the effects of imperfections on the results of the storey-based stability were studied by Ma & Xu (2019a), who concluded that they do not affect the results of the lateral stiffness equation, but rather influence the magnitudes of deflections causing premature failure due to excessive stresses in the materials.

3.4 Discussion of Shape Coefficients

In the proposed method, the use of assumed values of the shape coefficients v and w is recommended due to the transcendental relationships between these variables and the end fixity factors of the columns in the frame. Xu (2001) assumed $v_{FN,b} = 1$ for all beams in the storey-based stability method, in accordance to the assumption of asymmetrical buckling in the frame. Xu and Liu (2001) also demonstrated that the assumption of $v_{FN,b} = 1$ did not significantly affect the results of the storey-based stability method for single storeys. The asymmetrical buckling mode generally corresponds to the lateral sway failure mode consistent with the loss of lateral stiffness in an unbraced or semi-braced frame. In other words, asymmetrical bucking generally governs over other failure modes such as symmetrical buckling (Bažant and Xiang 1997). Similarly, Gil-Martín and Hernández-Montes (2012) and Li et al (2016) have all assumed $v_{FN} = 1$ for all members in their proposed methods of calculating the buckling loads and buckling length coefficients for sway frames, respectively. The alignment chart method also assumes asymmetric buckling for unbraced frames (Duan and Chen 1999). As such, the current study also proposes the use of $v_{FN} = 1$ for all members to provide an approximate solution to the lateral stiffness equation for each storey. As for w_{FN}, the previous storey-based stability formulations have all neglected the differential axial shortening of columns within the frames by assuming $w_{FN,b} = 0$ for beams and provided accurate results. As such, the same will be assumed in the proposed method. As for the columns, it will be shown that the assumption of asymmetrical buckling ($v_{FN} = 1$) effectively constrains w within finite values. Illustrated in Fig. 4 is a simplification of Fig. 3 in the typical buckled shape of a continually spliced column in the asymmetrical buckling mode. The chord rotation is ψ and the end rotations are θ_u and θ_l. With assuming asymmetrical buckling, let $\theta_u = \theta_l = \theta$, corresponding to $v_{ul} = v_{lu} = v = 1$. Define the following relationship:

$$\frac{\theta}{\psi - \theta} = k \tag{18}$$

In Eq. (18), k is the ratio between the end rotation, θ, to the angle between the chord and end rotation, ψ-θ. It would typically be expected that k can range from zero to infinity, with $k = \infty$ corresponding to the column end being aligned with the chord, and $k = 0$ corresponding to the column end being aligned with the vertical axis.

Fig. 4. Buckled shape of continually spliced column in the asymmetrical buckling mode

Although not impossible, negative values of k are rarely encountered as they would correspond to additional slope reversals and/or higher energy modes. With k typically ranging from zero to infinity, the value of $w_{ul} = w_{lu} = w$ is confined within the limits zero and unity via Eq. (19), which is the result of rearranging Eq. (18).

$$w = \frac{\psi}{\theta} = \frac{k}{k+1} \tag{19}$$

Finally, by inspection of Eq. (12) the effective rotational stiffness provided by the column decreases with respect to w, so taking $w = 1$ produces the most conservative result, while taking $w = 0$ produces the least conservative result and is only valid for braced frames whereby the deflection between storeys is zero. Therefore, it is recommended that in the proposed method, in lieu of more accurate analyses, $v = w = 1$ can be assumed to estimate the lower bound rotational stiffness of a column, and subsequently the lower bound critical loads of a frame. It is finally noted that this assumption of $v = w = 1$ also results in $R'_c = 0$ via substitution in Eq. (12), which is equivalent to neglecting the contribution of rotational stiffness from the columns altogether. The conservativeness of this assumption, as well as the sensitivity of the results of the proposed method to the values of the shape coefficients are further investigated in Section 5.

3.5 Column Rotational Buckling

It also should be noted that the lateral stiffness equation in Eq. (1a) becomes discontinuous when a column reaches its rotational buckling load, i.e. $N = N_u$ (Xu 2003), corresponding to the buckling load if the column were to be fully laterally braced. For most cases, this mode corresponds to $S_\Delta = -\infty$, and the lateral stiffness S_Δ monotonically decreases towards $-\infty$ as $N_{i,j}$ approaches $N_{u,i,j}$, as shown for a typical column in Fig. 5. In Fig. 5, β_0 is the value of β corresponding to $\phi = 0$.

Fig. 5. Typical lateral stiffness versus axial load plot; adapted from Ma and Xu (2019a)

The asymptotic relationship between S_Δ and the axial load can be explained by noting that a column that is fully braced from lateral sway will still buckle at the rotational buckling load (Xu 2001). As such, once the rotational buckling load is reached, it is impossible to maintain stability of the column, regardless of the amount of lateral bracing provided to the column. As S_Δ decreases towards negative infinity, the demand for lateral bracing stiffness from other columns in order to maintain stability of the column in the storey (i.e. $\Sigma S > 0$) increases towards infinity. The only exception to this behaviour, shown in Fig. 5, is for a column with $r_l = r_u$, whereby instability occurs at $N_i = N_{u,i,j}$ via a removable discontinuity as demonstrated in Ma and Xu (2019a). In such a case, S_Δ does not gradually decrease towards $-\infty$, as shown Fig. 5. Rather, at the removable discontinuity there is an instantaneous loss of

stiffness at the buckling load. In any case, for loads exceeding the rotational buckling load N_u, S_Δ can potentially return a positive value via Eq. (1) but would be invalid since rotational buckling has already occurred. Care should be taken to ensure that the rotational buckling load has not been exceeded during the analysis as it represents an upper bound for the column buckling load. According to Newmark (1949), the rotational buckling load of a column, N_u, can be approximated via Eq. (20). However, root-finding for the axial load during which the denominator in Eq. (1a) first reaches zero is required in order to obtain an exact solution.

$$N_u = \frac{\phi_u^2 EI}{L} \tag{20a}$$

$$\phi_u^2 \approx \frac{\pi^2}{K_{app}^2} = \pi^2 \left[\frac{\pi^2 + (12 - \pi^2) r_u}{\pi^2 + (6 - \pi^2) r_u} \right] \left[\frac{\pi^2 + (12 - \pi^2) r_l}{\pi^2 + (6 - \pi^2) r_l} \right] \tag{20b}$$

In Eq. (20), ϕ_u is the axial load coefficient corresponding to the rotational buckling load N_u, and K_{app} is an approximation of the effective length of the column. Note that the end fixity factors, r_u and r_l, are obtained from Eq. (2) with R based on Eqs. (15) as the connecting columns may be subject to lateral displacement. Note that a further discussion of the behaviour of the lateral stiffness equation during rotational buckling is included in Appendix A.

3.6 Computational Procedure

The following computational procedure can be used to estimate the critical loads of a multi-storey frame in accordance with the proposed decomposition method.

1. Input the constant parameters of the members in the frame (L, A, I, E_0, f_y), member-connection fixities (z), lateral bracing stiffness (K_b), and boundary conditions such as the end fixity factors corresponding to the column-to-ground connections ($r_{l,j}$ on Storey 1).
2. Assume that the most conservative case of asymmetrical buckling occurs ($v_{FN} = 1$ for all members, $w_{FN} = 1$ for columns and $w_{FN} = 0$ for beams).
3. Determine the proportional loading scheme and assign loads to the columns. Calculate the axial loads, N, in each column at each storey level.
4. Decompose the beams of the frame into equivalent rotational springs at the ends of the columns at each storey level via Eq. (15b).
5. Analyze each storey by calculating R'_c of the columns directly above and below the storey via Eq. (15c), summing the rotational stiffness via Eq. (15a), calculating the end fixity factors via Eq. (2) and then the lateral stiffness, ΣS, in Eqs. (1) or (17).

6. Increase the loads until the lateral stiffness of any single storey reaches zero, and record the corresponding critical loads.
7. Ensure that the rotational buckling load, N_u, in Eq. (20) has not been reached during the analysis. Otherwise, the loads corresponding to N_u represent the upper bound for the critical loads of the frame.

4 FEA Validation

The proposed method is by derivation an exact theoretical solution to account for nonlinear geometric effects (*P-Δ*), the accuracy of which is verified via the finite element analyses in this section. The equations associated with the proposed decomposition method were validated using ABAQUS. The critical loads of two example frames under proportional loading schemes were computed and compared with those obtained in ABAQUS. In each case, the calibrated values of the shape coefficients *v* and *w* obtained from the buckled shapes in the FEA were then used in the proposed equations to verify the exactness of the respective solutions.

4.1 Example 1

The first example is a two-storey (m = 2), two bay (n = 3) frame with rigid connections ($r_N = r_F = 1$ for all beams, and all columns continuously spliced) first introduced in Lui (1992) and subsequently adopted in Liu and Xu (2005) and Xu and Wang (2007) as a benchmark for verification and computational demonstration. The frame is shown in Fig. 6 and is loaded in proportion to the ratios shown at each node (i,j). For the purpose of comparison, the frame is assumed by all of the aforementioned researchers to behave elastically with E = 200 GPa and $I = 83.246\times10^6$ mm^4. The frame is fixed to the ground (r_u = 1). A finite element model of the frame was constructed in ABAQUS using B23 Euler-Bernoulli linear cubic wireframe elements, and the elastic buckling load was obtained by solving for the eigenvalues in the linear perturbation buckling step. The buckling loads of the frame total 112,470 kN in the finite element model, and the buckled shape of the frame is shown in Fig. 7.

Fig. 6. Two-bay, two-storey rigidly connected frame for Example 1

Fig. 7. Buckled shape in elastic buckling FEA of Example 1

From the buckled shape, it is observed that the deformations in the first storey are more severe compared to those of the second storey, suggesting the presence of a weak first storey. To verify the theoretical accuracy of the proposed equations of the proposed method in Section 3, calibrated values of the shape parameters (*v* and *w*) were obtained from the nodal rotations of the buckled shape in the finite element model, which were then used to calculate the end fixity factors for each column using the proposed method. The instability condition was determined by increasing

the loads proportionally until the lateral stiffness of either storey diminished to zero. The values of the calibrated shape parameters for the beams in the frame are presented in Table 1. The values of the calibrated shape parameters and end fixity factors during instability for each of the column in the frame are presented in Table 2.

Table 1. Calibrated beam shape parameters for Example 1

Table 2. Calibrated column shape parameters and end fixity factors for Example 1

The values in Table 2 marked with the (*) symbol correspond to shape parameters that are not needed for any of the calculations of the column end fixity factors but are included for the sake of completeness. The reason for this is that the shape parameters are only necessary for calculating R'_c via Eq. (15c), which is only required at the column splice at level $i = 1$. As such, the near end subscript N in calculating v_{FN} and w_{FN} corresponds to either the upper ends of the columns in Storey $i = 1$ (hence requiring v_{lu} and w_{lu}) or the lower ends of the columns in Storey $i = 2$ (hence requiring v_{ul} and w_{ul}). A form of asymmetrical buckling exists throughout the frame since all of the v_{FN} values are greater or equal to zero, indicating that the ends of the members rotate in the same direction – also apparently via observation of Fig. 7. Note that the negative value of r_l for Column (2,1) in Table 2 is the result of R'_c in Column (1,1) returning a negative value. It is possible for R'_c to become negative in some cases (Bridge and Fraser 1987), as the end moment M_i of a member is in actuality a function of all four deformation parameters, $\{\theta_i, \theta_j, y_i, y_j\}$, via Eq. (11), rather than just θ_i. R'_c is thus an effective value of the rotational stiffness which must also consider the rotation of the other end as well as the relative deflections on both ends. Nevertheless, it will be shown that carrying the negative values of R'_c through the analyses returns the correct critical loads corresponding to the instability condition. In some other situations, it can be seen in Eq. (12) that R'_c can also become negative if the columns are heavily loaded (high ϕ values), resulting in a dependency on the rotational stiffness of other members in order to maintain stability. This is similar to the concept of negative lateral stiffness in columns discussed in (Xu 2001). Based on the results, the first storey ($i = 1$) reached $(\Sigma S)_1 = 0$, becoming unstable when the total load reached 112,479 kN, while the second storey still maintained a residual lateral stiffness of $(\Sigma S)_2 = 3{,}580$ kN/m, as shown in Fig. 8. As such, it is confirmed that the first storey is a weak storey in this instability mode. Note that the values of the lateral stiffness may not be accurate at loads besides the critical load level since the calibrated values of the shape parameters only correspond to the critical load level, and are shown to change based on the loading in Appendix B.

Fig. 8. Decomposition method results for Example 1 with calibrated shape parameters constant

The difference in total load corresponding to the instability condition between the proposed method (with the calibrated shape parameters) and the FEA is therefore within 0.008%, which is virtually exact. As such, the equations from both the proposed method produce exact results when the calibrated shape parameters are used.

4.1.1 Comparison with Previous Method

For this example, it has been shown that the proposed equations of effective rotational stiffness produce exact results of the critical loads if the shape parameters are calibrated, and as such, are theoretically accurate. The Liu & Xu (2005) method, however, yields only approximate results. The critical load of the frame reported in Liu & Xu (2005) is only 108.2 MN, but involves several additional simplifications including the use of a Taylor series expansion to approximate the lateral stiffness, and $v_{FN} = 1$ for all members.

As such, some further work was required to appropriately compare the results based on the Liu & Xu (2005) method with the results of the proposed equations as follows. Repeating the Liu & Xu (2005) method but without adopting the Taylor series simplification and using the calibrated values of v_{FN} obtained from the FEA (instead of $v_{FN} = 1$) yields a critical total load of 132.6 MN, which is corresponds to an 18% error from both the FEA results and the proposed equations (both 112.5 MN). However, the critical load of 132.6 MN was obtained from calculating R'_c via Eq. (16), which was proposed in Liu & Xu (2005) and is inaccurate. If the corrected version of Eq. (16) shown in Eq. (15c) is used in the Liu & Xu (2005) method then the total critical load becomes 99.8 MN, which is still inaccurate compared to the proposed equations (112.5 MN), due to the remaining assumption of Eq. (5) adopted in the Liu & Xu (2005) method.

4.1.2 Simplified Analysis

The analysis of the two-bay, two-storey frame was repeated but with the proposed values of the shape parameters based on the most conservative asymmetrical buckling assumption discussed in Section 3.4 ($v_{FN} = 1$ for all members, $w_{FN} = 1$ for columns and $w_{FN} = 0$ for beams). The proposed decomposition method returns a critical total load of 114,487 kN using this assumption, which corresponds to an error of only 1.8% from the calibrated result. A further discussion of the errors related to the assumption of asymmetrical buckling under the proposed decomposition method is provided in Section 5.

4.2 Example 2

The second example is an original three-storey (m = 3), one-bay (n = 2) frame with semi-rigid beam-to-column connections ($Z = 25\times10^6$ Nm/rad for all beam-to-column connections) shown in Fig. 9.

Fig. 9. One-bay, three-storey semi-rigidly connected semi-braced frame for Example 2

Tension-only diagonal bracing of $K_b = 10^5$ N/m exists in either direction at each storey level (comparable to the lateral stiffness provided by a ¼" steel bar). All column splices are assumed to be continuous and the frame is rigidly connected to the ground (r_I = 1). The purpose of this example is to demonstrate the use of the proposed equations towards semi-braced frames with semi-rigid connections, in addition to applying the tangent modulus theory in Eq. (18). The proportional loading ratios are shown in Fig. 9 whereby $I = 83.246\times10^6$ mm^4, A = 7,420 mm^2, $E_0 = 2\times10^5$ MPa and f_y = 350 MPa. The slenderness ratios of the columns within the storey heights range from 55 to 86. Given this range of slenderness, the columns are in the range of inelastic buckling whereby the tangent modulus in Eq. (18) is applicable to the analysis. A finite element model of the frame was constructed in ABAQUS using B23 Euler-Bernoulli linear cubic wireframe elements, and the critical load was obtained by solving for the minimum eigenvalue in the linear perturbation buckling step. Due to the linear nature of the eigenvalue analysis, the values of the elastic modulus in each column needed to be manually entered based on the resulting critical loads. The total buckling load accounting for inelasticity obtained in the FEA converged to 4,885.70 kN, and the buckled shape in Fig. 10 corresponds to sway buckling.

Fig. 10. Buckled shape obtained from FEA for Example 2

To show that the frame is semi-braced, Fig. 11 illustrates the total buckling loads obtained by repeating the analysis in FEA with the value of K_{br} varied from 10^0 to 10^9 N/m.

Fig. 11. Buckling load obtained from FEA for varying lateral bracing stiffness, K_{br}

The plot in Fig. 11 is similar to the one shown in Ma and Xu (2019b), whereby a semi-braced frame is defined as having a critical load within the transition zone shown. For values of K_{br} to the left of the transition zone, the critical load is not significantly affected by the lateral bracing and the frame can be treated as unbraced. Similarly, for values of K_{br} to the right of the transition zone, the critical load approaches the rotational buckling load corresponding to braced frames. Although the limits of the transition zone are not officially defined, $K_{br} = 10^5$ N/m is clearly within the transition zone as the critical load of 4,885.70 kN is well in between the unbraced critical load (4,599 kN) and rotational buckling load (5,366 kN). Also, note that according to CSA S16 (CSA 2014), a frame with bracing may be considered as fully braced if its sway stiffness is at leaset five times greater than that obtained with

485 the bracing removed. In the absence of the bracing K_{br}, the first storey would have the lowest lateral stiffness at
486 5.23×10^5 N/m (approximated with assuming $v_{FN} = 1$ for all members, $w_{FN} = 1$ for columns, $w_{FN} = 0$ for beams).
487 Thus, adding the bracing of $K_{br} = 10^5$ N/m to the first storey results in a lateral stiffness only 1.19 times that of the
488 frame without bracing, demonstrating that the frame is semi-braced.
489 The proposed decomposition method was utilized to confirm the buckling load of the frame using the calibrated
490 values of the shape parameters obtained from the FEA and based on the buckling shape shown in Fig. 10. Fig. 12
491 plots the computed values of decomposed storey-based lateral stiffness, ΣS, for the three storeys. However, the
492 calibrated shape parameters, v_{FN} and w_{FN}, are held constant and independent of the increasing loads, when in reality
493 they vary depending on the loads and cannot be easily determined due to the transcendental relationships, shown in
494 Appendix B. This assumption results in inaccurate values of the storey lateral stiffness at loads other than the critical
495 load. In other words, unless the shape parameters are derived at each load level, the results in Fig. 12 cannot be
496 relied upon at any load level other than the critical load. In fact, the trend of increasing lateral stiffness with load for
497 Storeys 2 and 3 in Fig. 12 does not make sense. For this reason, as is one of the purposes of this section, it is
498 demonstrated that use of the calibrated parameters is not recommended for practice, and only serves to validate the
499 proposed method. As discussed in Section 3.4 and shown later in Section 5, the adoption of the standard
500 asymmetrical buckling assumption produces more reliable and practical results. To be clear, the values of the
501 calibrated shape parameters used to plot Fig. 12 were taken based on the buckled shape in FEA corresponding to a
502 total critical load of 4,885.70 kN.
503 **Fig. 12.** Decomposition method results for Example 2 with shape parameters constant and corresponding to the
504 critical load

505 In Fig. 12, the decomposition method correctly identifies the instability of the first storey with a total load of exactly
506 4,885.70 kN (exact to the FEA result). As discussed previously, the plotted behaviour of Storeys 2 and 3 at load
507 levels other than the critical load is inaccurate because the shape parameters v and w for the members of the frame
508 are not constant and actually vary based on the magnitudes of the applied loads. Especially, in cases such as this
509 example where the tangent elastic modulus and column end fixity factors can change dramatically with increases to
510 the applied loads via Eq. (18), the values of the shape coefficients will be highly influenced by the load level. As
511 such, the lateral stiffness plot in Fig. 12 may be highly inaccurate at any load level other than the failure load of
512 4,885.7 kN, to which the shape parameters are calibrated. The lateral stiffness of zero indicating the failure of Storey

1 shown at the total load of 4,885.7 kN in Fig. 12, however, is valid and correct since the calibrated shape parameters correspond to that loading level.

It can also be observed that R'_c in Eq. (15c) can even become arbitrarily negative if inaccurate values of the shape parameters are adopted. As the calibrated values of the shape parameters cannot easily be determined at any given loading level, a simplification is necessary for the proposed decomposition method to be of any use in practice. It will be shown in the following sections that if the assumption of asymmetrical buckling discussed in Section 3.4 is adopted, the lateral stiffness of the storeys will always decrease with the applied loading, unlike the behaviour shown in Fig. 12, while maintaining an acceptable degree of accuracy. As such, the asymmetrical buckling assumption is recommended over the use of calibrated or otherwise estimated shape parameters in the proposed method as the later can lead to inaccurate results.

4.2.1 Simplified Analysis

With assuming the most conservative case of asymmetrical buckling (v_{FN} = 1 for all members, w_{FN} = 1 for columns and w_{FN} = 0 for beams), the analysis of the three-storey frame in Fig. 9 was repeated using the proposed method. The resulting total critical load was 4,876.48 kN, as shown in Fig. 13.

Fig. 13. Un-calibrated analysis results of proposed decomposition method for Example 2

As expected and shown in Fig. 13, the lateral stiffness of the storeys decrease monotonically with applied loading under this assumption. Using the assumed shape parameters in this case resulted in an error of only 0.2% to the critical load (4,885.70 kN obtained from the calibrated analysis). The simplified analysis also correctly predicts the presence of a weak first storey in this case.

5 Parametric Analyses

The purpose of this section is to investigate the sensitivity of the shape parameters to the solution of the proposed method in determining the critical loads of multi-storey frames. Two studies are conducted on the frame in Example 1. The first study assesses the effect of varying the shape parameters on the elastic critical total load of the frame under the original proportional loading case. The second study is a stochastic analysis that investigates the error associated with assuming the most conservative case of asymmetrical buckling shape of the frame discussed in Section 3.4 (v_{FN} = 1 for all members, w_{FN} = 1 for columns and w_{FN} = 0 for beams) while randomly varying the properties of the frame. The main focus of the study is on the effect of the *w* factor, since a parametric study on *v* has

already been conducted by Xu and Liu (2002), which concluded that using values of v_{FN} from -1.0 to 1.0 generally has an insignificant effect on the critical loads of frames and thus provides good estimates of the results.

5.1 Effect of Varying Shape Parameters on Example 1

Given that the proposed method should ideally be usable without needing to calibrate the shape parameters via FEA, some preliminary values of the shape parameters are assumed in a reanalysis of the frame in Example 1. Asymmetrical elastic buckling corresponding to the sway failure mode is assumed with $v_{FN} = 1$ for all members. Let $w_{FN} = w_{NF} = w_0$ bounded between zero and unity for each column, as consistent with the conclusion of Section 3.4. In this parametric study, w_0 is constant for all of the columns in the frame. The resulting lateral stiffness is plotted versus the total load in the frame for the applicable values of w_0 incremented by 0.2 in Fig. 14.

Fig. 14. Product of storey lateral stiffness versus total load with varying w_0

As observed in Fig. 14, the total load of the frame during elastic instability varies between 114.5 MN and 118.3 MN, with the most conservative estimate at $w_0 = 1$ and the least conservative estimate at $w_0 = 0$. These results are consistent with the conclusion in Section 3.4 that $w_0 = 1$ is the most conservative simplification. However, since the critical load of the frame reported in the previous section is 112.5 MN, assuming $w_0 = 1$ still overestimates the critical load by 1.8%, while $w_0 = 0$ results in a 5.2% overestimation of the critical total load. The overestimation is due to the assumption of the asymmetrical buckling shape in the beams via $v_{FN,b} = 1$, while the bounds for w_0 only apply to the buckled shapes of the columns. As such, the error in estimation of the critical loads due to assuming $v_{FN,b} = 1$ accounts for the overestimation of the critical load. Underestimations and overestimations of the critical load resulting from assuming $v_{FN,b} = 1$ were also observed in Xu and Liu (2002).

Note that if asymmetrical buckling is not assumed then w_{ul} and w_{lu} cannot be bounded within reasonable limits. Further discussion regarding the conservativeness of assuming the most conservative case of asymmetrical buckling is provided in Section 5.2. Nevertheless, this assumption still provides a reasonably accurate estimate of the critical total load (within 1.8% error) for the frame in Example 1.

5.2 Stochastic Error Analysis

In order to assess the sensitivity of the errors in the total loads corresponding to the instability condition that can potentially be encountered with assuming the most conservative case of asymmetrical buckling, some of the properties of frame in Example 1 were randomly varied in a stochastic analysis. 1,000 randomized realizations of the frame were created. In each realization, the moment of inertia of the columns and beams were randomly selected

between 1.0 I to 11.0 I via a uniform distribution. The beam-to-column rotational stiffness (Z) was randomly selected from zero to 10^8 Nm/rad via a uniform distribution. Each column-to-ground connection also had its rotational stiffness ($R_{l,1,j}$) randomly selected from 10^1 to 10^{12} Nm/rad, with the exponent being uniformly distributed. Finally, the values of the proportional applied loading ratios at each storey level of each column were randomly distributed between zero and unity. In each realization, the elastic critical load was obtained via FEA and with using the proposed method. Each of the finite element models were set up in a similar way to that described in Section 5.1. The error between the results was compared using Eq. (22).

$$\text{Error} = \frac{P_{cr,prop} - P_{cr,FEA}}{P_{cr,FEA}} \times 100\% \tag{22}$$

In Eq. (22), $P_{cr,prop}$ is the critical total load obtained via the proposed method and $P_{cr,FEA}$ is the critical load obtained via the eigenvalue buckling analysis in ABAQUS. A negative error corresponds to a conservative underestimation of the critical load using the proposed method, while a positive error corresponds to an un-conservative overestimation of the critical load using the proposed method. Based on the 1,000 test cases, a histogram of the errors calculated via Eq. (22) is plotted in Fig. 15.

Fig. 15. Difference between critical loads under the most conservative asymmetrical buckling assumption versus FEA

The mean error from the sample data was -5.6%, showing in the majority of cases the proposed method underestimates the critical load. The standard deviation was 14.8%, with 78.6% of the sample data within one standard deviation (from -20.3% to +9.3%) and 96.5% of the sample data within two standard deviations of the mean (from -35.2% to +24.1%). Based on the 1,000 data samples, the 95% confidence intervals for the mean and standard deviation were between -6.5% and -4.6% for the mean, and between 14.2% and 15.5% for the standard deviation, indicating that the mean and standard deviations are reliable. The critical load was underestimated by over 25% only 5.5% of the time, while the critical load was overestimated by over 10% only 11.6% of the time. The reason that the critical load is sometimes overestimated despite assuming $w_{FN,c} = 1$ is due to the error associated with assuming the values of $v_{FN,b}$, which were demonstrated in both Section 5.1 and (Xu and Liu 2002) to potentially result in slight overestimations or underestimations of the critical loads. Note also that if the analyses in this section were repeated for Example 2, the errors would be generally be expected to decrease as the introduction of the tangent modulus causes the elastic modulus to decrease very quickly and the critical load becomes less sensitive to

595 the shape parameters. This is exemplified in the simplified analysis of Example 2 in Section 5.2, where the error as a
596 result of using the assumed shape parameters was within 0.1%, as well as in some further analyses conducted in Ma
597 (forthcoming). Anyway, from the results of this parametric study it can be concluded that assuming the most
598 conservative case of asymmetrical buckling ($v = 1$ for all members, $w = 1$ for columns and $w = 0$ for beams) can
599 provide reasonable and generally conservative estimates of the critical load of a sway frame.

600 **6 Conclusion**

601 A frame decomposition method for evaluating the stability of multi-storey, semi-rigidly connected steel sway frames
602 has been established. Idealized connections can also be analyzed using the proposed method as they correspond to
603 special cases of semi-rigid connections. As soon as the lateral stiffness of any individual storey diminishes to zero,
604 the frame is considered to be unstable. The proposed equations for calculating the lateral stiffness are shown to be
605 theoretically accurate upon comparison with FEA results. Practically, the proposed method can be used to identify
606 the critical loads and the weakest storey in a frame, defined as the first storey that reaches a lateral stiffness of zero.
607 The solutions of the proposed decomposition method are sensitive to the shape of the buckling mode, which is
608 difficult to solve and may be assumed. The method involves adopting a set of buckling shape parameters derived in
609 this paper which can be used to approximate the critical loads within reasonable accuracy. The assumption of the
610 worst case of asymmetrical buckling in the sway mode is recommended as it provides good estimates for the lower
611 bound critical loads of the frames, demonstrated via parametric studies and numerical examples. Based on the
612 results of the parametric studies, the critical loads of the example frames can be reasonably estimated via the most
613 conservative asymmetrical buckling assumption, with errors between -20.3% to +9.3% occurring in 78.6% of the
614 test cases. A negative error corresponds to an underestimation of the critical load, whereas a positive error
615 corresponds to an overestimation of the critical load. Therefore, the proposed decomposition method produces
616 accurate approximations of the critical loads when the asymmetrical buckling assumption is adopted. It is finally a
617 theoretical advancement in storey-based buckling, adding to the knowledge and background that is crucial towards
618 the future development of future storey-based stability methods. The proposed shape parameters make it possible to
619 simplify and quantify the contribution of all connected members at the ends of a column as equivalent rotational
620 springs.

621 **Data Availability Statement**

Some or all data, models, or code generated or used during the study are available from the corresponding author by request. These include the scripts used to run the numerical examples, all finite element validation models and ABAQUS input files used in the stochastic error analysis.

Acknowledgements

The authors wish to thank the National Science and Engineering Research Council of Canada (NSERC) (RGPIN-203154-2013) for the financial support of this work.

References

1. AISC (American Institute of Steel Construction). 2017. *Steel Constructional Manual*. Chicago, IL: AISC.
2. Bahaz, A., Amara, S., Jaspart J, P. and Demonceau, J. F. 2017. "Analysis of the behaviour of semi rigid steel end plate connections". *MATEC Web of Conferences*, 02058,1-6.
3. Bažant, Z. P. and Xiang, Y. 1997. "Postcritical imperfection-sensitive buckling and optimal bracing of large regular frames". *J Struct Eng*, 123(4), 513-522.
4. Bridge, R. Q. and Fraser, D. J. 1987. "Improved G-factor method for evaluating effective lengths of columns". *J Struct Eng*, 113(6), 1341-1358.
5. CSA (Canadian Standards Association). 2014. *Design of Steel Structures*. CSA S16. Toronto, ON: CSA Group.
6. Duan, L. and Chen, W. F. 1999. "Effective Length Factors of Compression Members". *Structural Engineering Handbook*, Boca Raton: CRC Press LLC.
7. Georgios, E. M. and Gantes, C. J. 2006. "Buckling strength of multi-story sway, non-sway and partially-sway frames with semi-rigid connections". *J Constr Steel Res*, 62, 893-905.
8. Gil-Martín, L. M. and Hernández-Montes, E. 2012. "Unified buckling length coefficient for sway and non-sway structures". *Eng Struct*, 40(2012), 436-444.
9. Gunaydin, A. and Aydin, R. 2019. "A simplified method for instability and second-order load effects of framed structures: Story-based approach". *Struct Des Tall Spec*, 28(4), 1-23.
10. Hellesland, J. 2009. "Extended second order approximate analysis of frames with sway-braced column interaction". *J Constr Steel Res*, 62, 893-905.
11. Hellesland, J. and Bjorhovde, R. 1996. "Improved frame stability analysis with effective lengths". *J Struct Eng*, 122(11), 1275-1283.

12. Kim, N-I. and Choi, D-H. 2015. “System buckling analysis for multi-story frames subjected to nonconservative forces”. *Int J Steel Struct*, 15(2), 285-297.
13. LeMessurier, W. 1977. “A practical method of second order analysis Part 2 – Rigid Frames”. *Eng J*, 14(2), 49-67.
14. Li, Q., Zou, A. and Zhang, H. 2016. “A simplified method for stability analysis of multi-story frames considering vertical interactions between stories”. *Adv Struct Eng*, 19(4), 599-610.
15. Liu, Y. and Xu, L. 2005. “Storey-based stability analysis of multi-storey unbraced frames”. *Struct Eng Mech*, 19(6), 679-705.
16. Lui, E. M. 1992. “A novel approach for K factor determination”. *Eng J*, 29, 150-159.
17. Ma, T. 2020. *The Storey-Based Stability of Steel Frames Subjected to Variable Gravity and Fire Loading* (PhD Thesis), University of Waterloo, Waterloo, ON.
18. Ma, T. and Xu, L. 2019a. “Effects of column imperfections on capacity of steel frames in variable loading”. *J Constr Steel Res*, 165(2020), 105819.
19. Ma, T. and Xu, L. 2019b. “The stability of semi-braced steel frames containing members with stepped segments”. In *Proceedings of the SDSS 2019 International Colloquium on Ductility of Steel Structures*, 727-734, Prague, Czechia.
20. Ma, T. and Xu, L. 2019c. Shear deformation effects on stability of unbraced steel frames in variable loading. *J Constr Steel Res*, 164(2020), 105811.
21. Meghezzi-Larafi, I. and Tati, A. 2016. “The effective length estimation of columns in semi-rigid jointed braced frames”. *Journal of Applied Engineering Science Technology*, 2(2), 91-97.
22. Monforton, G. and Wu, T. 1963. “Matrix analysis of semi-rigidly connected frames”. *J Struct Div*, 89(6), 13-42.
23. Newmark, N. 1949. “A simple approximate formula for effective end-fixity of columns”. *Journal of Aeronautical Sciences*, 16(2), 116.
24. Teresa Guevara-Perez, L. 2012. “‘Soft story’ and ‘weak story’ in earthquake resistant design: A multidisciplinary approach”. In *15th World Conference on Earthquake Engineering 2012*, Lisbon, Portugal.
25. Webber, A., Orr, J. J., Shepherd, P. and Crothers, K. 2015. “The effective length of columns in multi-storey frames”. *Eng Struct*, 102, 132-143.

26. Xu, L. 2001. “The buckling loads of unbraced PR frames under non-proportional loading”. *J Constr Steel Res*, 58, 443-465.
27. Xu, L. 2003. “A NLP approach for evaluating storey-buckling strengths of steel frames under variable loading”. *Struct Multidicip O*, 25(2003), 141-150.
28. Xu, L. and Liu, Y. 2001. “Story stability of semi-braced steel frames*”. J Constr Steel Res*, 58(2002), 467-491.
29. Xu, L. and Liu, Y. 2002. “Storey-based effective length factors for unbraced PR frames”. *Eng J*, 39(1), 13-29.
30. Xu, L. and Wang, X.H. 2007. “Stability of multi-storey unbraced steel frames subjected to variable loading”. *J Constr Steel Res*, 63(2007), 1506-1514.
31. Yura, J. A. and Helwig, T. A. 2005. *Bracing for stability*. AISC and SSRC.
32. Yura, J. A. 1971. “The effective length of columns in unbraced frames”. *Eng J*, 8(2), 37-42.
33. Ziemian, R. 2010. *Guide to Stability Design Criteria for Metal Structures*, Wiley & Sons Ltd.

Appendix A Behaviour of β

The β coefficient introduced in Eq. (1) is a modifier to the lateral stiffness of a column which accounts for the effects of the axial force (ϕ) and end connections (r_u and r_l). Its behaviour is studied in Ma (2020) and summarized in this appendix. In Figs. A.1 and A.2, the value of β is plotted with respect to the ϕ (proportional to $N^{0.5}$) and varying end fixity factors.

Figure A.1 – Behaviour of β with respect to ϕ and r_u with r_l = 1 (adopted from Ma 2020)

Figure A.2 – Behaviour of β with respect to ϕ and r_u with r_l = 0 (adopted from Ma 2020)

When β diminishes to zero, the column no longer offers resistance and begins to lean on the system. This occurs earlier for lower values of the end fixity factors. Of course, for a pinned-pinned column ($r_l = r_u = 0$), the column has no lateral stiffness (β=0 in Fig. A.2). In contrast, a fixed-fixed column ($r_l = r_u = 1$) begins to lean when $\phi = \pi$. The maximum value of β for columns in compression is unity, as shown in Fig. A.1, and corresponds to a lateral stiffness of $12EI/L^3$ for the column. Note that for the purpose of this paper tensile loads can be conservatively represented using $\phi = 0$. A derivation for the expression of β with respect to tensile loads is included in Ma (2020).

Finally, the plots of β become discontinuous at the rotational buckling load, discussed in Section 3.5 and studied in Ma (2020). The rotational buckling load is the load at which a fully-braced column with the same end conditions buckles. A laterally-braced pinned-pinned column ($r_l = r_u = 0$) buckles when $\phi = \pi$, while the same phenomenon occurs for a laterally-braced fixed-fixed column when $\phi = 2\pi$.

Appendix B Expressions of Shape Coefficients

Exact expressions of the shape coefficients in the rotational stiffness equation with considering the effects of axial loads are presented in the derivation of the proposed method are derived in this appendix. Consider first the deformed shape of a semi-rigidly connected column in Fig. B.1 resulting from axial load N and lateral load Q.

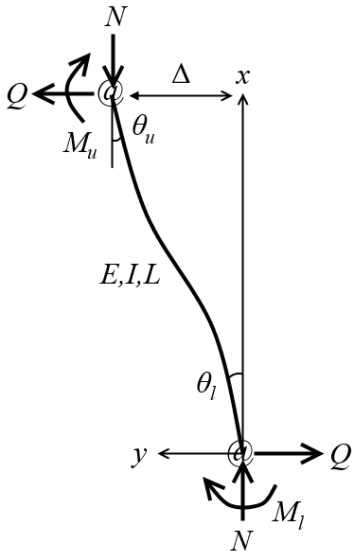

Figure B.1 – Semi-rigidly connected column subjected to axial and lateral load

By applying the external equilibrium of forces and moments, the following relation can be obtained.

$$M_l + M_u = N\Delta + QL \tag{B.1}$$

With assuming that the semi-rigid connections behave linearly, the end moments are given in Eq. (B.2).

$$M_l = \theta_l R_l \tag{B.2a}$$

$$M_u = \theta_u R_u \tag{B.2b}$$

The internal bending moment is expressed via the Euler-Bernoulli equation in Eq. (B.3).

$$-EIy'' = -M_l + Qx + Ny \tag{B.3}$$

Substituting Eq. (B.2a) into Eq. (B.3) and solving the differential equation for *y* yields Eq. (B.4).

$$y(x) = C_1 \cos\left(\frac{\phi}{L}x\right) + C_2 \sin\left(\frac{\phi}{L}x\right) + \frac{\theta_l R_l}{N} - \frac{Q}{N}x \tag{B.4}$$

There are four boundary conditions for Eq. (B.4), which are listed in Eq. (B.5).

$$y(0) = 0 \tag{B.5a}$$

$$y(L) = \Delta \tag{B.5b}$$

$$y'(0) = \theta_l \tag{B.5c}$$

$$y'(L) = \theta_u \tag{B.5d}$$

Substituting Eq. (B.5) into Eq. (B.4) and Eq. (B.2) into Eq. (B.1) provides five equations which are used to solve for the variables Δ, θ_l, θ_u, C_1 and C_2 in terms of all other variables. The resulting expressions for Δ, θ_l, and θ_u are thus presented in Eq. (B.6).

$$\Delta = \frac{QL^3}{\phi^3 EI}\left[\frac{18r_l r_u - a_3\cos\phi + (a_1 - a_2)\phi\sin\phi}{a_1\phi\cos\phi + a_2\sin\phi}\right] \tag{B.6a}$$

$$\theta_u = \frac{QL^2(1-r_u)}{\phi EI}\left[\frac{(1-r_l)\phi\sin\phi + 3r_l(1-\cos\phi)}{a_1\phi\cos\phi + a_2\sin\phi}\right] \tag{B.6b}$$

$$\theta_l = \frac{QL^2(1-r_l)}{\phi EI}\left[\frac{(1-r_u)\phi\sin\phi + 3r_u(1-\cos\phi)}{a_1\phi\cos\phi + a_2\sin\phi}\right] \tag{B.6c}$$

The shape coefficients v and w can therefore be expressed via Eq. (B.7) as follows:

$$v_{ul} = \frac{\theta_u}{\theta_l} = \left[\frac{1-r_u}{1-r_l}\right]\left[\frac{(1-r_l)\phi\sin\phi + 3r_l(1-\cos\phi)}{(1-r_u)\phi\sin\phi + 3r_u(1-\cos\phi)}\right] \tag{B.7a}$$

$$v_{lu} = \frac{\theta_l}{\theta_u} = 1/v_{ul} \tag{B.7b}$$

$$w_{ul} = \frac{\Delta}{L\theta_l} = \frac{18r_l r_u - a_3\cos\phi + (a_1 - a_2)\phi\sin\phi}{\phi^2(1-r_l)\left[(1-r_u)\phi\sin\phi + 3r_u(1-\cos\phi)\right]} \tag{B.7c}$$

$$w_{lu} = \frac{\Delta}{L\theta_u} = w_{ul}/v_{ul} \tag{B.7d}$$

Note that Eq. (B.7) is valid as long as the column end rotation is equal to the rotation of the end of the connecting column (i.e. $\Phi = 0$ in Fig. (2)), since by definition the shape coefficients are functions of the end rotations, θ, outside of the connection shown in Fig. 3, rather than the end rotation of the current column, θ-Φ. This requirement is satisfied when $z_u = z_l = 1$, which is globally satisfied if the columns are continuously spliced, as per the discussion in Section 3.1. Note also that rearranging for Q/Δ in Eq. (B.6a) yields S_Δ in Eq. (1a), the lateral stiffness of the column derived in (Xu 2001). Similarly, define $S_{\theta,u}$ and $S_{\theta,l}$ as the stiffness against rotation at the upper and lower column ends with respect to the lateral force Q, in Eq. (B.8).

$$S_\Delta = \frac{Q}{\Delta} = \frac{\phi^3 EI}{L^3}\left[\frac{a_1\phi\cos\phi + a_2\sin\phi}{18r_l r_u - a_3\cos\phi + (a_1 - a_2)\phi\sin\phi}\right] = \frac{12EI}{L^3}\beta \tag{B.8a}$$

$$S_{\theta,u} = \frac{Q}{\theta_u} = \frac{\phi EI}{L^2(1-r_u)}\left[\frac{a_1\phi\cos\phi + a_2\sin\phi}{(1-r_l)\phi\sin\phi + 3r_l(1-\cos\phi)}\right] \tag{B.8b}$$

$$S_{\theta,l} = \frac{Q}{\theta_l} = \frac{\phi EI}{L^2(1-r_l)}\left[\frac{a_1\phi\cos\phi + a_2\sin\phi}{(1-r_u)\phi\sin\phi + 3r_u(1-\cos\phi)}\right] \tag{B.8c}$$

Finally, for beams, $v_{FN,b}$ must be calculated with respect to the rotations of the connected columns and is thus derived in Eq. (B.9), as consistent with the assumption that all columns in the frame have the same deflection.

$$v_{FN,b} = \frac{\theta_{u,F}}{\theta_{u,N}} = \frac{Q_F / S_{\theta,u,F}}{Q_N / S_{\theta,u,N}} = \frac{\Delta S_{\Delta,F} / S_{\theta,u,F}}{\Delta S_{\Delta,N} / S_{\theta,u,N}} = \frac{S_{\Delta,F} / S_{\theta,u,F}}{S_{\Delta,N} / S_{\theta,u,N}} \tag{B.9}$$

In Eq. (B.9), Q_F and Q_N are the portions of an arbitrarily applied lateral load Q at the top of the storey partitioned among the columns of the frame, and F and N refer to the far-end and near-end columns. The shape parameters in Eq. (B.7) and Eq. (B.9) are exact but cannot easily be solved due to being transcendental in r_u and r_l of the columns.

Table 1. Calibrated beam shape parameters for Example 1

Beam (i,j)	v_{RL}	w_{RL}	w_{LR}
(1,1)	0.17	0.00	0.00
(1,2)	3.60	0.00	0.00
(2,1)	6.95	0.00	0.00
(2,2)	0.02	0.00	0.00

Table 2. Calibrated column shape parameters and end fixity factors for Example 1

Column (i,j)	v_{ul}	v_{lu}	w_{ul}	w_{lu}	r_u	r_l
(1,1)	∞*	0.00	∞*	1.78	0.683	1.00
(1,2)	∞*	0.00	∞*	10.5	0.945	1.00
(1,3)	∞*	0.00	∞*	2.93	0.838	1.00
(2,1)	0.01	67.2*	0.45	30.5*	0.915	-0.560
(2,2)	0.62	1.63*	2.69	4.38*	0.854	0.853
(2,3)	0.00	336.1*	0.75	242.6*	0.995	0.709

* Denotes a value that was not needed in any of the computations